Wilson, P. R., Cinar, A. F., Mostafavi, M., & Meredith, J. (2018). Temperature Driven Failure of Carbon Epoxy Composites: A Quantitative Full-field Study. *Composites Science and Technology*, *155*, 33-40. https://doi.org/10.1016/j.compscitech.2017.11.020

Temperature Driven Failure of Carbon Epoxy Composites – A Quantitative Full-field Study

P. R. Wilson[1], A. F. Cinar[2(a)], M. Mostafavi[3] and J. Meredith[2(b)]

[1]International Manufacturing Centre, University of Warwick, Coventry, CV4 7AL

[2]Department of Mechanical Engineering, The University of Sheffield, Sir Frederick Mappin Building, Sheffield, S1 3JD, United Kingdom

[3]Queen's Building, University of Bristol, University Walk, Clifton BS8 1TR

Email: [1]p.wilson.5@warwick.ac.uk, [2(a)]afcinar1@sheffield.ac.uk, [3]m.mostafavi@bristol.ac.uk [2(b)]j.meredith@sheffield.ac.uk

1 Abstract

Aerospace composites are exposed to low temperatures that induce high levels of stress within the material. This is sufficient to induce fractures and eventually delaminations and failure. Thus, understanding how these temperature induced translaminar fractures can be reduced is an important area of research.

This work investigates cross-ply unidirectional (UD) and woven (W) carbon fibre laminates with MTM46 epoxy to assess how the cure schedule (low temperature, LTC and high temperature, HTC) effect temperature driven fractures. A novel digital image correlation technique was applied to determine in-situ fracture progression versus temperature. Thermal techniques investigated the degree of cure, resin plasticity, thermal expansion and beta transition effects.

The cure schedule for carbon epoxy laminates has a marked effect on quantity of manufacturing induced fractures and the temperature at which temperature induced internal fracture occurs. This work has demonstrated that a lower temperature cure is more robust against temperature driven fracture despite having a larger coefficient of thermal expansion (CTE) and similar levels of plasticity. Low temperatures induce high

internal stresses but the residual stress resulting from high temperature cure is of greater concern.

DIC is an excellent method to determine onset and progression of translaminar fracture as well as the behaviour of composite materials subject to temperature effects. This work is of great benefit when considering the design of CFRP structures subject to low temperature loading, furthermore the data can be used to more accurately model this phenomena in future.

Keywords: Carbon fibres; Low temperature failure; Residual stress; Digital image correlation; Oven cure;

2 Introduction

Unidirectional (UD) prepreg carbon fibre reinforced polymers (CFRP) possess superior in plane mechanical properties to woven systems and offer large weight savings in mass critical sectors such as aerospace. UD prepregs are inherently anisotropic possessing fibre dominated longitudinal strengths of greater than 2000 MPa but comparatively poor resin dominated transverse strengths of approximately 30 MPa [1]. This, in combination with the widely differing longitudinal (-0.3×10^{-6} °C^{-1}) and transverse (30×10^{-6} °C^{-1}) linear coefficient of thermal expansion (CTE) [2] leads to residual stress within the laminate which can surpass the transverse strength of the ply leading to transverse crack formation [3-6].

These cracks reduce the modulus of the laminate [4, 7], act as stress concentrators, provide a pathway to freeze thaw cracking [8, 9]. Consequently, the management of residual stress in cross ply laminates is critical in aerospace CFRP components which operate at -56.5 °C at an altitude of 12 km [10]. Potential solutions include the use of off axis fibres laminated to introduce compliance and manage out of plane loading. Another

option is the use of toughening agents within the epoxy matrix to limit the residual stress within the laminate [4] and increase the thermal stability [11, 12], however these do not fully prevent microcracking. Other researchers have demonstrated that a reduction in the degree of cure (α) for an epoxy system has been shown to increase fracture toughness from approximately 1 to 1.25 K_I/K^o_I by reducing the α from 100 to 60% [13]. Within a composite system the optimum epoxy degree of cure has been shown to depend on the mechanical property being measured [14, 15]. For a Fiberite T300/976 carbon epoxy system the 0° tensile modulus varied from 172.4, 179.3, 182.7 to 175.8 MPa with a α of 60, 70, 80 and 90% respectively [14]. Furthermore, reducing degree of cure has been shown to significantly lower residual stress within the laminate [6, 16].

Epoxy systems possess a low temperature energy dissipation mechanism, typically over the range -120 to 20 °C [17, 18] which are known as a beta transition. These beta transitions correspond to the reduction in molecular mobility at low temperatures and have been shown to play a role in the toughness of the epoxy system [17, 19]. There is no evidence of a link between beta transition and fracture toughness although it is known to cause a reduction in plasticity and is therefore suggested to have an effect on low temperature behaviour. This work will investigate the low temperature behaviour of a commercial epoxy and assess if it exhibits any changes in resin plasticity with respect to temperature. It will also assess if there is a link between the temperature at which composite fracture is induced and the reduction in molecular mobility of the epoxy system at sub ambient temperatures.

Fractures in CFRP have been analysed using a wide array of techniques such as optical microscopy [6, 20-22], acoustic emission [5], speckle pattern interferometry [23, 24] and in-situ microscopy [3, 7], digital image correlation (DIC) [25] and X-ray

tomography [20, 25] to name a few. Thermally induced fractures in CFRP are either a post fracture analysis, which enables a quantification of fractures or in situ fracture analysis gathering fracture temperatures and/or fracture quantification. Optical microscopy [6, 20-22] and X-ray tomography [20] have been used as post fracture techniques for analysis of thermally stressed laminates. In situ methods for low temperature loading of samples have included optical microscopy [3, 26, 27] acoustic emission [28] and dynamic mechanical analysis [29]. These low temperature in situ techniques offer information of the fracture temperature and in the case of optical microscopy can offer quantification of cracks, but they are analytically intensive and produce limited information on the fracture progression. DIC is a simpler route to gathering rich data on the development of laminate cracks. DIC analyses the changes in sequential images of a textured surface during deformation to produce a surface strain field. This enables time based visualisation and quantification of crack formation. It has been used by many researchers to measure the crack length and opening displacement profile in a range of materials [30].

This work presents a novel in-situ approach for analysing thermally induced crack formation in CFRP laminates via the application of DIC. The data rich nature of the DIC technique enables formation of the crack opening displacement (COD) via a custom Matlab script, providing a detailed analysis of translaminar fracture and delamination in UD and woven CFRP samples. The work will utilise the results of this novel application to analyse the effects of degree of cure on the laminates resilience against thermally induced fracture.

3 Experimental

3.1 Materials and manufacture

Samples were manufactured using two pre-impregnated fabrics: a 660 gsm unidirectional (UD) with Pyrofil™ HR40 (Misubishi Rayon Carbon) fibres and medium temperature moulding MTM46 (Cytec ltd) resin and a 660 gsm 2x2 twill with HTA40 (Toho Tenax) fibres also with MTM46. Samples were cured with either a high temperature cure (HTC), maximum 180 °C or a low temperature cure (LTC), maximum 120 °C as defined in Table 1 [31]. The LTC cure represents a part cured from low temperature tooling in which a cooling step is required to remove the tool before final post-cure whilst, the HTC represents a more traditional high temperature tooling typically used in aerospace components. 400 mm x 400 mm panels were laid up on a 770NC Frekote (Henkel, Germany) mould released aluminium sheet. Debulking was performed every four plies for 15 minutes at room temperature (20°C) to aid consolidation. Samples were then cured under vacuum using either the LTC or HTC schedule.

Two layups were used for cryogenic fracture analysis, one composed solely of UD fibres and the other a typical aerospace layup designed to be robust against temperature driven fracture with a UD central core surrounded by woven material. A UD layup of $[90_3, 0]_s$ was chosen as previous work has shown it to be particularly susceptible to temperature driven fracture [3]. The UD samples were designated UD-LTC and UD-HTC with a cured laminate thickness of 5.2 ±0.1 mm. The woven/UD layup used the following schedule [±45W, 0/90W, 0,90W, 0 UD, 0/90W, 0/90W, ±45W] where W corresponds with woven plies. The resulting cured laminates were designated W-LTC and W-HTC with a cured laminate thickness of 5.1 ±0.1 mm.

For thermal expansion measurements, panels of 10 off 0° plies measuring 100 mm x 100 mm of the UD and woven MTM46 were laminated using the same procedure as above. Each panel was cured using the LTC and HTC schedule and designated UD HTC CTE, UD LTC CTE, WHTC CTE and WLTC CTE laminate.

3.2 Differential scanning calorimetry (DSC)

Degree of cure (α) was determined using a differential scanning calorimeter (DSC1 - Mettler Toledo Ltd, UK) equipped with an automatic sample changer. Samples of uncured MTM46 HR40 prepreg, UD LTC and UD HTC panels were powdered using a cryomill (Retsch, Germany) to produce a homogeneous powder. 5 – 10 mg of each sample were sealed in 40 µL aluminium pans with a pierced lid. Samples were isothermally held for 2 hours at 250 °C until the samples had fully cured. The enthalpy of cure was determined via integration of the normalised heat flow with respect to time over the first hour using Origin (OriginLabs Corp., USA). α was calculated using the formula below [32]:

$$\alpha = \frac{(\Delta H_t - \Delta H)}{\Delta H_t} \times 100 \quad (1)$$

Where ΔH_t is the total enthalpy of reaction in $J.g^{-1}$ from the uncured prepreg, whilst ΔH is the enthalpy of reaction.

3.3 Coefficient of thermal expansion (CTE)

Samples were cut from the UD HTC CTE, UD LTC CTE, WHTC CTE and WLTC CTE panels using a diamond-coated blade along the fibre axis into 5 mm x 5 mm x 5 mm cubes with a linear precision saw (Isomet 5000 – Buehler, Ltd). Two samples from each panel were polished using 1200 grit carbide paper followed by a 9 µm and 6 µm diamond suspension polish (MetaDi, Buehler, UK) to ensure the samples were parallel.

Each was then tested using a Diamond Thermomechanical analysis (TMA) (Perkin and Elmer Ltd, UK) using a silica probe with 4 kPa force and a temperature ramp from 20 to 80 ºC at 5 ºC.min^{-1} in air. The mean coefficient of linear thermal expansion $\overline{\alpha}$ was taken between 40 and 60 ºC using the following equation [33].

$$\overline{\alpha} = \frac{\Delta L}{\Delta T} \times \frac{1}{L_0} \qquad (2)$$

Where L_0 is the original length ΔL is the change in length and ΔT is the change in temperature.

3.4 Dynamic mechanical thermal analysis (DMTA)

Dynamic mechanical thermal analysis (DMTA) was performed using a Tritec 2000 (Triton Ltd, UK) to investigate the role of degree of cure on the beta and glass transition. Samples with dimensions 50 × 2 x panel thickness (mm) were cut from the UD HTC CTE and UD LTC CTE laminates along the fibre axis and dried at 50 ºC under vacuum for 2 days. These were tested in three point bending mode using a multi frequency of 1 and 10 Hz from -100 to 275 ºC with a heating rate of 2 ºC.min^{-1} cooled with liquid nitrogen (LN_2). Samples were thermally cycled twice to verify if features were due to residual cure or material parameters, the resulting scans were designated as 1st and 2nd cycle.

3.5 Cryogenic fracture analysis

Six samples of 50 mm x 50 mm were cut from each panel (UD LTC, UD HTC, WLTC and WHTC). Each sample was polished along the cut edge such that the centre ply was orientated with the fibre ends facing the polished face as shown in Figure 1. This was to visualise transverse microcracking of the central ply and to ensure the surface was level for the camera. Samples were polished using 1200 grit carbide paper followed by a 9

µm and 6 µm diamond suspension polish (MetaDi, Buehler, UK). A matt white base coat and matt black speckle pattern was applied to the polished sample face using Deco Art Crafters acrylic paint (DecoArt Inc. USA). Samples were tested 2 months after laminate production and stored in standard lab conditions at 20 °C.

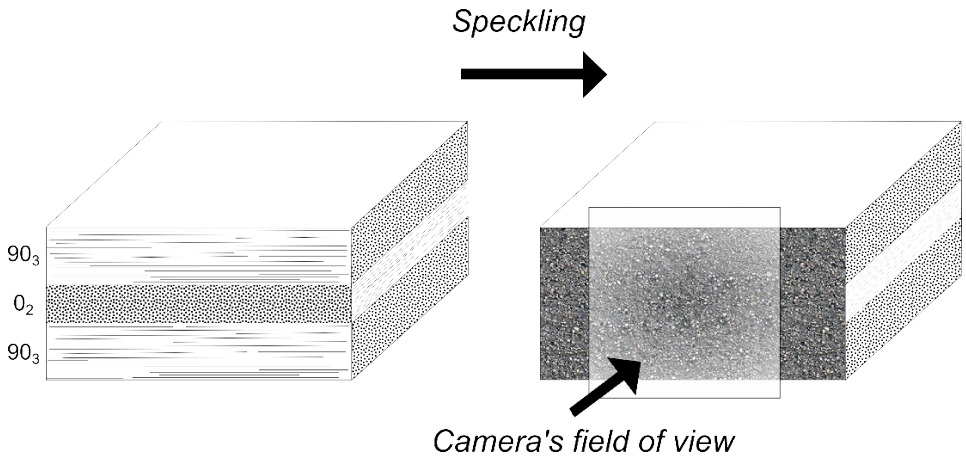

Figure 1 Side view of polished panels and cameras field of view

3.5.1 Experimental setup

Digital Image Correlation (DIC) was performed as shown in Figure 2 using a LaVison Ltd DIC kit which consisted of a Imager E-lite 5M camera 5 Mega pixel camera with 2.45 K x 2 K pixel resolution and a pixel size of 3.45 µm x 3.45 µm with LED lamps. The camera was levelled and aligned to the samples surface using a circular sprit level and rulers. Samples were supported in the environmental chamber using a matt black painted aluminium block to reduce reflections. A Tokina AT-X Pro D 100mm F2.8 macro lens was set to an aperture of F8 to maximize focus whilst maintaining an appropriate depth of field. Calibration was performed using a glass calibration plate with a grid of 0.25 mm dots (LaVison ltd, UK). Post calibration, samples were placed into the field of view to match the calibration. From here the samples were taped to the block using a temperature resistant tape (Flashbreaker 1, Tygavac Ltd, UK) to prevent the sample moving during the introduction of LN_2. A T-type thermocouple was taped to

the upper surface of the sample to enable accurate temperature logging at low temperature. The thermocouple was converted into a voltage readout using a TXDIN1620 thermocouple to analogue converter (Omega Ltd, UK). The temperature voltage readout was added as an analogue input into Davis (LaVision Ltd, UK) for sequential temperature logging with image capture.

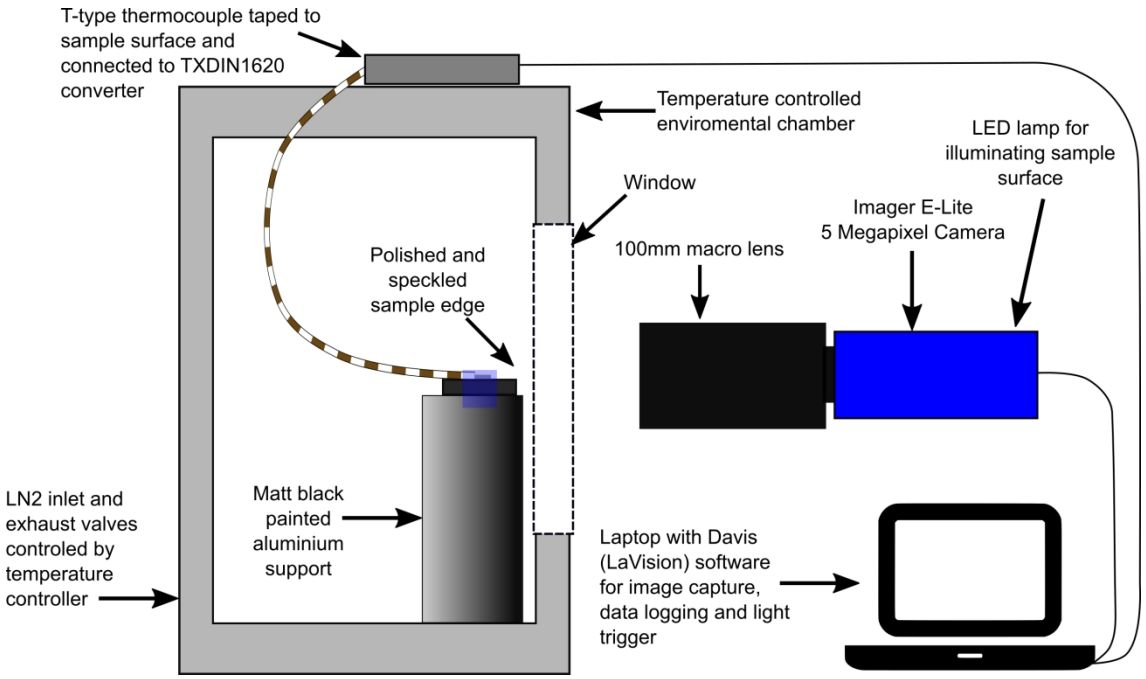

Figure 2 Experimental set for low temperature loading and digital image correlation

Recording of images and temperature were set to 0.5 Hz. Samples were then dwelled at 60 °C for 1 hour to homogenize the sample temperature and reduce moisture. The chamber temperature was then set to -100 °C and LN2 cooling, temperature logging and image capture commenced. Logging was stopped once samples had reached a temperature of -85 °C as this was the lowest temperature in which the sample chamber could reach before the cooling rate fell below 10 °C.min^{-1}.

3.5.2 DIC analysis

Davis version 8.2.3 (LaVision Ltd, UK) DIC software was used to determine the surface displacements and crack formation and propagation. In order to carry out such analysis, shift correction and intensity normalisation were used to remove sample shift due to aluminium sample holder contractions, sample and camera vibration. A 256 pixel area for shift correction was placed centrally at the top of the image allowing subpixel level shifts. The centre top was chosen due to low deformation for each sample. Image correlation was performed using the least squares matching method with seeding points inset from the top and bottom of the laminate to account for laminate fracture.

The resulting displacement field was exported and using a custom Matlab script, crack detection and horizontal average crack opening was determined. The code automatically detects the discontinuity in the displacement field and uses the vectors outside of the discontinuous region to determine the COD. This was calculated by subtracting the displacement vector from each subset displacements on opposite sides of the crack. This was then averaged across the crack for each image.

DIC calibration was tested over the experimental range of temperatures to investigate any variations in the window and experimental setup. The calibration process was repeated at 40 ºC intervals and the standard deviation of the process varied approximately 0.3 pixels. The pixel to mm conversion factor at this temperature range was 284.7±1.697 pixel/mm. This can be interpreted as a displacement measurement accuracy of 1μm for calibration and 6μm for temperature change.

4 Results and discussion

4.1 DSC

The baseline subtracted normalised heat flow for each sample set is given in Table 2. The mean enthalpy of reaction for each sample set was used in equation (1) resulting in a degree of cure of 64.03 % for LTC and 83.22 % for HTC samples for a 250 °C cured system as shown in Table 2.

4.2 DMTA

The storage modulus and tan δ of UD LTC and UD HTC samples are highlighted in Figure 3. On the first run the UD LTC and UD HTC samples increase their storage modulus at 100 and 125 ºC respectively which is the onset of cure. The repeat cycle on both LTC and HTC samples provide no increase in storage modulus at 100 and 125 ºC demonstrating that the increase in storage modulus during the initial run is due to residual cure. Both LTC and HTC cure schedules produce an under-cured laminate as shown in Table 2. The increase in storage modulus from residual cure prevents determination of the glass transition temperature for our samples. The peak tan δ for the fully cured samples were 180.8 ºC (1 Hz) and 188.25 ºC (10 Hz) for LTC and 179.05 ºC (1 Hz) and 185.86 ºC (10 Hz) for HTC.

In both the LTC and HTC systems during the initial and repeat runs the modulus is reduced as the sample is heated up from -100 ºC. This modulus reduction is expected due to increased chain mobility. Over the -100 to 50 ºC range two beta relaxation events are observed in the tan δ. This doublet corresponds to an increase in loss modulus with respect to the increase in storage modulus, which is commonly correlated to activation side chain mobility and crank rotation of aromatic groups [34]. Both LTC and HTC samples show a similar magnitude of their beta relaxation, which upon heating to 275

ºC and repeating the DMTA the beta is diminished. This corresponds to crosslink density having an effect on the magnitude of the beta relaxation. The similar magnitudes in beta for HTC and LTC systems are expected to allow equal levels of plasticity in each system upon cooling.

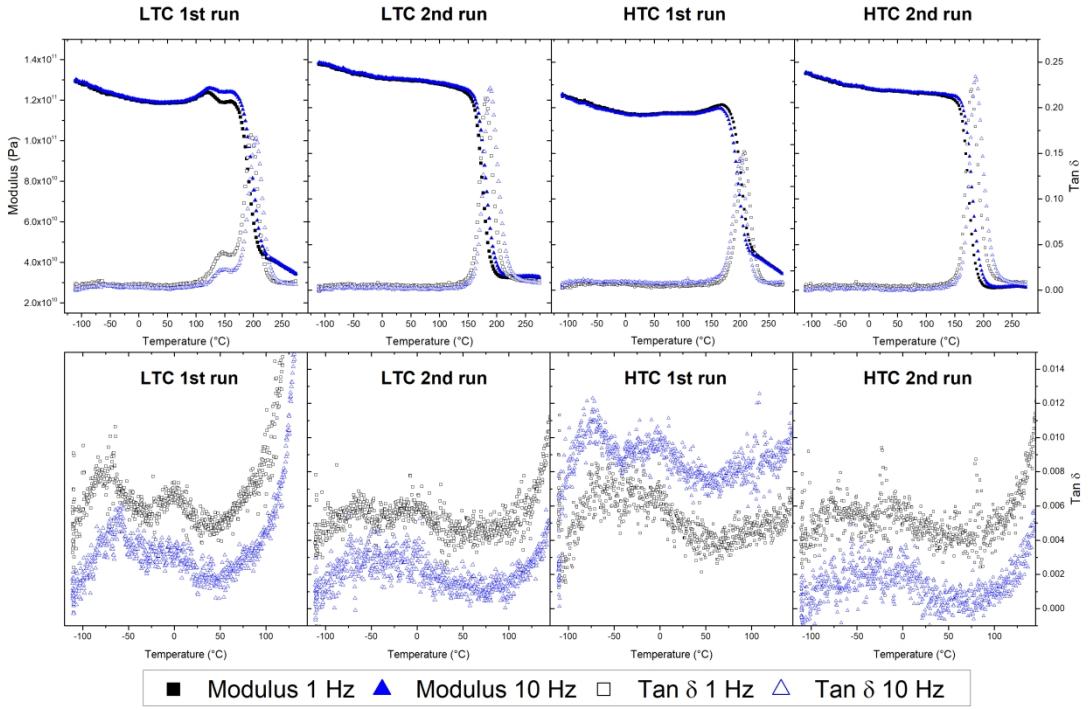

Figure 3 DMTA data of the LTC and HTC samples on their first and second heating cycles. Lower graph shows lower beta transitions in the tan δ.

4.3 Coefficient of thermal expansion (CTE)

CTE values for the constituent materials are shown in Table 3. In all cases the thermal expansion is greatest in the LTC systems when compared with the HTC systems which is in line with literature and is due to a reduction in chain mobility in the HTC system [35, 36]. The greatest difference in CTE is between the UD 0º and 90º plies. Both systems had a fibre dominated 0º CTE of -1.6 x 10^{-6} ºC^{-1}. The resin dominated 90º CTE

demonstrated that the higher crosslink density in the HTC system was 72.6% of the LTC CTE, 41.04 x 10-6 ºC^{-1} versus 56.71 x 10-6 ºC^{-1}.

4.4 Cryogenic fracture analysis

4.4.1 Crack opening displacement (COD) plots

The principal strain field images for each sample from 0 to -80 °C are shown in Figure 4 demonstrating the transverse fractures and delaminations. Figure 5 highlights the COD for each of the six samples per laminate (UD LTC, UD HTC, W LTC and W HTC) with respect to temperature.

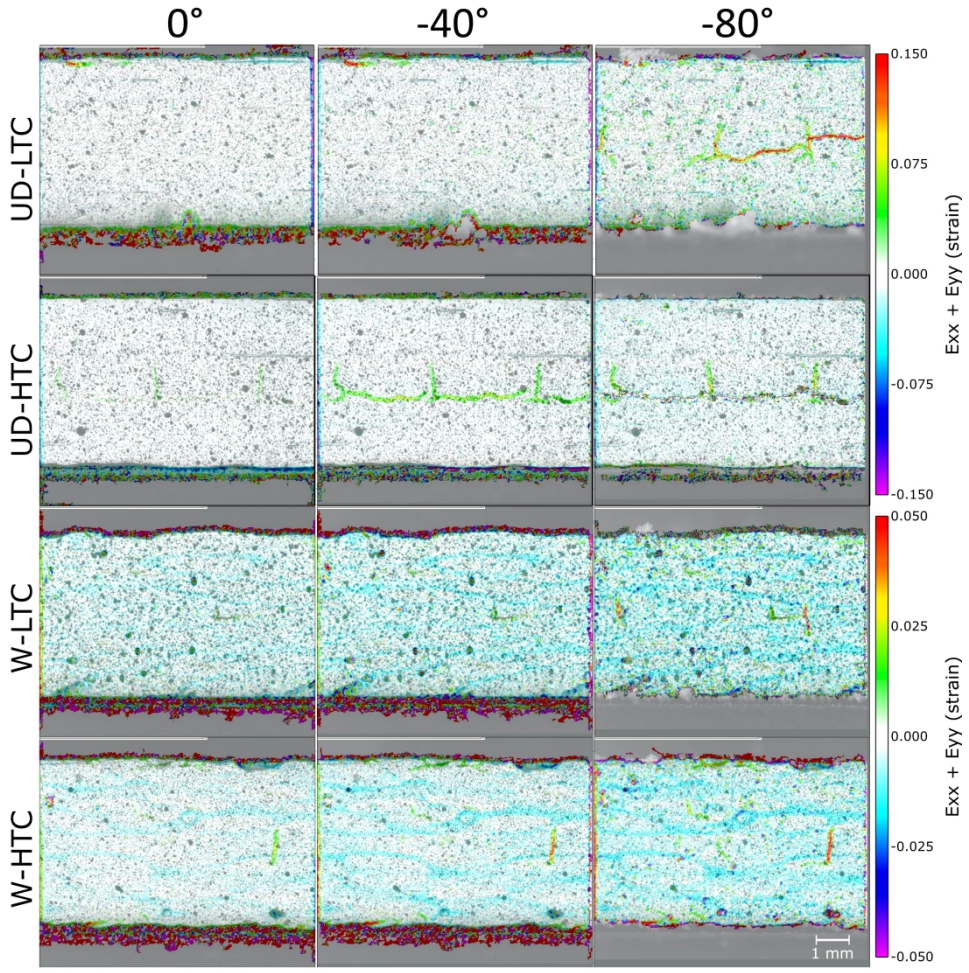

Figure 4 Principal strain field images from Davis for UD-LTC, UD-HTC, W-LTC and W-HTC from 0 to -80 C

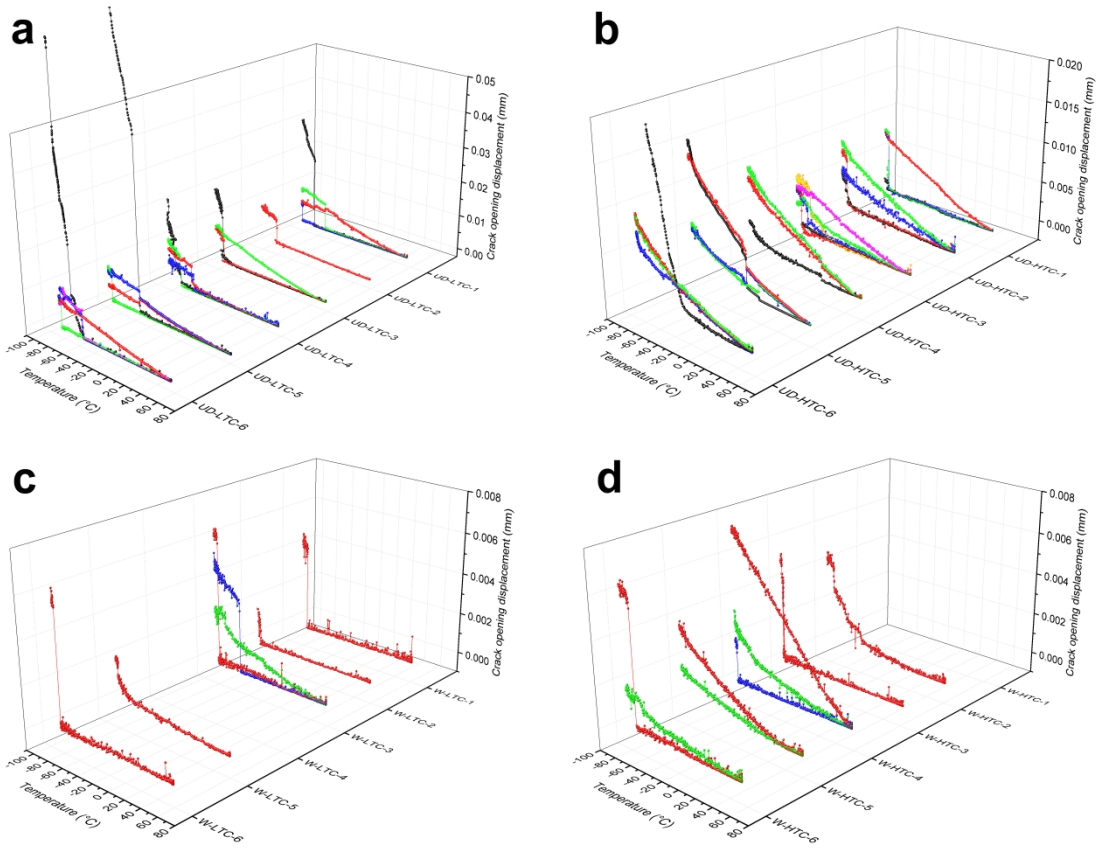

Figure 5 Crack opening displacement versus temperature for a) UD-LTC, b) UD-HTC c) W-LTC and d) W-HTC. Black markers represent delamination's whilst all other colours represent transverse cracks

All laminate types in this study were found to transverse fracture during cooling. Delamination only occurred within UD laminates due to the high levels of CTE mismatch. Laminates followed one of two trends; either a sudden fracture at a particular temperature designated as a "temperature induced fracture" or a gradual crack opening from the start of the experiment designated as an "existing fracture". The number of fractures of each crack type are shown in Figure 6.

The data displayed in Figure 5 and Figure 6 demonstrates that UD laminates have a greater number of transverse cracks compared to woven laminates. It is also apparent that the HTC schedule leads to an increase in total number of transverse cracks for both

UD and woven laminates. Finally, the HTC schedule has higher levels of existing fractures formed during manufacture.

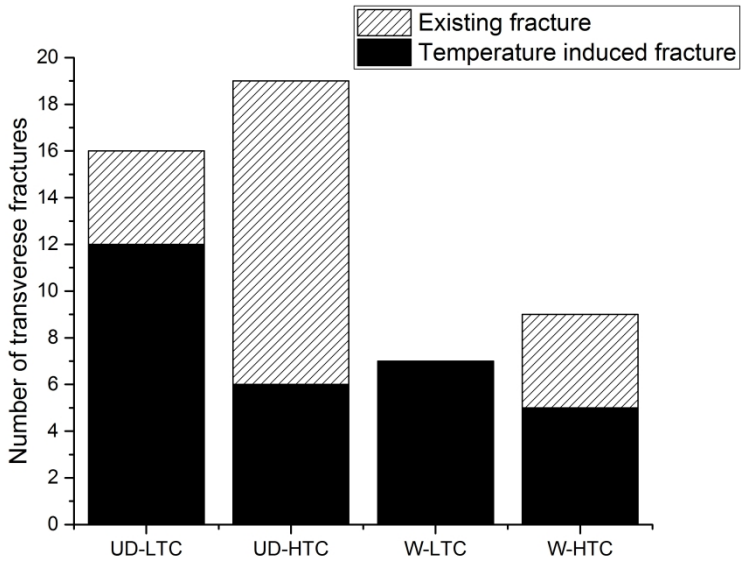

Figure 6 Frequency and type of transverse fractures in UD-LTC, UC-HTC, W-LTC and W-HTC laminates

Higher levels of thermally induced stress are expected within LTC laminates due to higher CTE mismatch between plies combined with similar levels of resin plasticity versus HTC laminates. However, Figure 5 and Figure 6 demonstrate the opposite relationship highlighting that the higher temperature cure induces higher residual stress and consequently more manufacturing induced fractures occur.

The output from DIC analysis had some noise that prevented the use of peak differentiation to determine the cracking onset temperature. As such these were determined manually by extracting the first instance of an inflection in the COD versus temperature data. Samples where no inflection was observed i.e. existing cracks, were not used to calculate the mean cracking temperature. The cracking temperatures for each laminate are presented in Table 4.

The average delamination temperature for UD-HTC was -33.9 ºC versus -61.8 ºC for UD-LTC which is significant since -33.9 ºC is within the normal operating window of most aerospace components. This is especially important when the range of delamination temperatures are considered. For the UD-HTC the highest temperature at which delamination occurred was 11.2 ºC versus -52.5 ºC for UD-LTC. The early delamination of UD-HTC laminates at 11.2 ºC produced a larger standard deviation of 40 ºC for the delamination temperatures of UD-HTC laminates. This variability in UD-HTC samples relates to the higher residual stress in UD-HTC laminates, as the larger residual stress is distributed across the laminate a higher variability in sample fracture temperature occurs. This suggests that the larger CTE mismatch between plies in lower degree of cure laminates is less problematic than the increase in residual stress in HTC schedules.

UD-LTC laminates initially transverse crack whereas UD-HTC laminates tended to delaminate in favour of further transverse cracking which had occurred during manufacture as shown in Figure 5. The mean transverse fracture and delamination temperatures in UD-LTC systems are -59.8 and -61.8 ºC respectively. When compared with DMTA results in Figure 3 these temperatures correspond to the point where the resin has passed through the initial peak in tan δ corresponding to a reduction in resin plasticity. The overall increase in crack frequency, manufacturing induced transverse cracks and higher temperature delamination in UD-HTC demonstrates that residual stress is a more significant factor in thermal induced fracture as opposed to the reduced CTE produced upon further resin curing.

Woven laminates showed a significant reduction in the crack frequency compared to UD laminates. W-LTC laminates possessed no manufacturing induced transverse cracks and transverse cracks appeared at a slightly higher temperature in W-HTC laminates.

There is minimal difference in mean cracking temperature between W-LTC and W-HTC. However, when data from Figure 5 and Figure 6 are considered, it is apparent that there are a greater number of fractures occurring in the W-HTC laminates. It is evident that the W-HTC samples have manufacturing induced transverse cracks whereas the W-LTC laminates do not but, subsequently they are more resilient to thermally driven fracture. As with the UD laminates the fracture temperature corresponds to the point within the DMTA where the molecular mobility has reduced and is partially through the second low temperature transition. Whilst the beta transition may play a role in the fracture temperature of laminates the residual stress is a larger contributing factor, causing premature failure in UD-HTC laminates prior to matrix stiffening.

5 Conclusions

MTM46 cross ply laminates cured at 120 °C (LTC) and 180 °C (HTC) have a degree of cure of 64.03 % and 83.22 % respectively. A beta transition for the MTM 46 resin was apparent from -100 to 50 °C and shows minimal change with degree of cure until it is fully cured suggesting LTC and HTC laminates have similar levels of resin plasticity.

The UD 0° (fibre dominated) CTE varies from -1.59 to -1.62 $x10^{-6}$ $ºC^{-1}$, the UD 90° (matrix dominated) varies from 41.04 to 56.71 $x10^{-6}$ $ºC^{-1}$. The woven materials had a 0° CTE from 4.47 to 8.56 $x10^{-6}$ $ºC^{-1}$ again with the low temperature cure having the larger CTE. The CTE at 45° was from 5.14 to 9.04 $x10^{-6}$ $ºC^{-1}$ which is directly comparable demonstrating quasi-isotropic thermal expansion. Both the woven and UD laminates with a low temperature cure have a higher CTE than the corresponding laminates with a high temperature cure. This is due to the lower levels of crosslink density.

The average delamination temperature for UD-HTC was -33.9 ºC versus -61.8 ºC for UD-LTC. The UD-LTC laminates initially transverse crack whereas the UD-HTC

laminates tended to delaminate in favour of further transverse cracking. The UD-HTC laminates have more transverse cracks than UD-LTC and a greater percentage are manufacturing induced. It was also apparent that the HTC schedule leads to an increase in total number of transverse cracks for both UD and woven laminates. UD laminates have a greater number of transverse cracks compared to woven laminates. The W-LTC and W-HTC did not delaminate and showed a mean transverse fracture temperature of -74.4 ºC and -71.5 ºC respectively demonstrating their resilience against temperature induced fracture.

The cure schedule for carbon epoxy laminates has a marked effect on quantity of manufacturing induced fractures and the temperature at which temperature induced internal fracture occurs. This work has demonstrated that a lower temperature cure is more robust against temperature driven fracture despite the larger CTE and similar levels of plasticity exhibited. This will induce higher internal stresses but the residual stress produced by the high temperature cure is of greater concern.

DIC is an excellent method to determine onset and progression of translaminar fracture as well as the behaviour of composite materials subject to temperature effects. In order to improve on this method it will be necessary to consider a volumetric analysis using techniques that can non-destructively examine the interior of the material e.g. X-ray tomography.

This work is of great benefit when considering the design of CFRP structures subject to low temperature loading, furthermore the data can be used to more accurately model this pheonomena in future.

ACKNOWLEDGEMENTS

We gratefully acknowledge the support of Hybrid Air Vehicles limited and Innovate UK (101798) as part of the LOCATE project in funding this work. Forward composites are acknowledged for the manufacture of panels.

REFERENCES

1. Advance-composites-group. *MTM46 intermediate service temperature vacuum processable prepreg*. Composites House, Sinclair Close, Derbyshire, DE757SP, UK. 2005.
2. Hancox, N.L., *Thermal effects on polymer matrix composites: Part 1. Thermal cycling.* Materials & Design, 1998. **19**(3): p. 85-91.
3. Adams, D.S., D.E. Bowles, and C.T. Herakovich, *Thermally Induced Transverse Cracking in Graphite-Epoxy Cross-Ply Laminates.* Journal of Reinforced Plastics and Composites, 1986. **5**(3): p. 152-169.
4. Varna, J., et al., *A Study of the Opening Displacement of Transverse Cracks in Cross-Ply Laminates.* International Journal of Damage Mechanics, 1993. **2**(3): p. 272-289.
5. Bailey, J.E., P.T. Curtis, and A. Parvizi, *On the Transverse Cracking and Longitudinal Splitting Behaviour of Glass and Carbon Fibre Reinforced Epoxy Cross Ply Laminates and the Effect of Poisson and Thermally Generated Strain.* Proceedings of the Royal Society of London. A. Mathematical and Physical Sciences, 1979. **366**(1727): p. 599-623.
6. Timmerman, J.F., B.S. Hayes, and J.C. Seferis, *Cure temperature effects on cryogenic microcracking of polymeric composite materials.* Polymer Composites, 2003. **24**(1): p. 132-139.

7. Sebaey, T.A., et al., *Measurement of the in situ transverse tensile strength of composite plies by means of the real time monitoring of microcracking.* Composites Part B: Engineering, 2014. **65**: p. 40-46.

8. Dutta, P.K. and D. Hui, *Low-temperature and freeze-thaw durability of thick composites.* Composites Part B: Engineering, 1996. **27**(3): p. 371-379.

9. Shi, J.-W., et al., *Tensile behavior of FRP and hybrid FRP sheets in freeze–thaw cycling environments.* Composites Part B: Engineering, 2014. **60**: p. 239-247.

10. Cavcar, M., *The international standard atmosphere (isa).* Anadolu University, Turkey, 2000. **30**: p. 9.

11. Nettles, A.T., *Low Temperature Mechanical Testing of Carbon-Fiber/Epoxy-Resin Composite Materials*. 1996: National Aeronautics and Space Administration, Marshall Space Flight Center.

12. He, Y.-x., et al., *Micro-crack behavior of carbon fiber reinforced thermoplastic modified epoxy composites for cryogenic applications.* Composites Part B: Engineering, 2013. **44**(1): p. 533-539.

13. Tang, J. and G.S. Springer, *Effects of Cure and Moisture on the Properties of Fiberite 976 Resin.* Journal of Composite Materials, 1988. **22**(1): p. 2-14.

14. Johnson, J.B. and C.N. Owston, *The effect of cure cycle on the mechanical properties of carbon-fibre/epoxide resin.* Composites, 1973. **4**(3): p. 111-117.

15. Lee, S.-Y. and G.S. Springer, *Effects of Cure on the Mechanical Properties of Composites.* Journal of Composite Materials, 1988. **22**(1): p. 15-29.

16. White, S.R. and H.T. Hahn, *Cure Cycle Optimization for the Reduction of Processing-Induced Residual - Stresses in Composite Materials.* Journal of Composite Materials, 1993. **27**(14): p. 1352-1378.

17. Szyndler, M.W., et al., *Multifunctional deoxybenzoin-based epoxies: Synthesis, mechanical properties, and thermal evaluation.* Polymer, 2014. **55**(17): p. 4441-4446.

18. Williams, J.G., *The beta relaxation in epoxy resin-based networks.* Journal of Applied Polymer Science, 1979. **23**(12): p. 3433-3444.

19. Eftekhari, M. and A. Fatemi, *On the strengthening effect of increasing cycling frequency on fatigue behavior of some polymers and their composites: Experiments and modeling.* International Journal of Fatigue, 2016. **87**: p. 153-166.

20. Grogan, D.M., et al., *Damage characterisation of cryogenically cycled carbon fibre/PEEK laminates.* Composites Part A: Applied Science and Manufacturing, 2014. **66**: p. 237-250.

21. Bechel, V.T., M. Negilski, and J. James, *Limiting the permeability of composites for cryogenic applications.* Composites Science and Technology, 2006. **66**(13): p. 2284-2295.

22. Timmerman, J.F., B.S. Hayes, and J.C. Seferis, *Cryogenic Microcracking of Carbon Fiber/Epoxy Composites: Influences of Fiber-Matrix Adhesion.* Journal of Composite Materials, 2003. **37**(21): p. 1939-1950.

23. Loukil, M.S., J. Varna, and Z. Ayadi, *Damage Characterization in Glass Fiber/Epoxy Laminates Using Electronic Speckle Pattern Interferometry.* Experimental Techniques, 2015. **39**(2): p. 38-45.

24. Zrida, H., et al., *Crack opening displacement determination in damaged cross-ply laminate using electronic speckle pattern interferometry (ESPI).* IOP Conference Series: Materials Science and Engineering, 2012. **31**(1): p. 012002.

25. Goidescu, C., et al., *Damage investigation in CFRP composites using full-field measurement techniques: Combination of digital image stereo-correlation,*

infrared thermography and X-ray tomography. Composites Part B: Engineering, 2013. **48**: p. 95-105.

26. Ju, J. and R.J. Morgan, *Characterization of Microcrack Development in BMI-Carbon Fiber Composite under Stress and Thermal Cycling.* Journal of Composite Materials, 2004. **38**(22): p. 2007-2024.
27. Ajaja, J. and F. Barthelat, *Damage accumulation in a carbon fiber fabric reinforced cyanate ester composite subjected to mechanical loading and thermal cycling.* Composites Part B: Engineering, 2016. **90**: p. 523-529.
28. Kumagai, S. and Y. Shindo, *Experimental and Analytical Evaluation of the Notched Tensile Fracture of CFRP-Woven Laminates at Low Temperatures.* Journal of Composite Materials, 2004. **38**(13): p. 1151-1164.
29. Timmerman, J.F. and J.C. Seferis, *Predictive modeling of microcracking in carbon-fiber/epoxy composites at cryogenic temperatures.* Journal of Applied Polymer Science, 2004. **91**(2): p. 1104-1110.
30. Mostafavi, M. and T.J. Marrow, *In situ observation of crack nuclei in poly-granular graphite under ring-on-ring equi-biaxial and flexural loading.* ENGINEERING FRACTURE MECHANICS, 2011. **78**(8): p. 1756-1770.
31. Poulsen, H.F., et al., *Measuring strain distributions in amorphous materials.* Nat Mater, 2005. **4**(1): p. 33-36.
32. Sichina, W.J. *Characterization of Epoxy Resins Using DSC*. 2000. 4.
33. ISO, *11359-2:1999 Plastics -- Thermomechanical analysis (TMA) -- Part 2: Determination of coefficient of linear thermal expansion and glass transition temperature*. 1999.
34. Menard, K.P., *Dynamic mechanical analysis: a practical introduction*. 2008: CRC press.

35. Kravchenko, O.G., et al., *Prediction of the chemical and thermal shrinkage in a thermoset polymer.* Composites Part A: Applied Science and Manufacturing, 2014. **66**: p. 35-43.

36. Zarrelli, M., A.A. Skordos, and I.K. Partridge, *Investigation of cure induced shrinkage in unreinforced epoxy resin.* Plastics, Rubber and Composites, 2002. **31**(9): p. 377-384.

LIST OF FIGURES

Table 1 Low and high temperature cure cycles

Low temperature cure (LTC)	**High temperature cure (HTC)**
Ramp at 2 °C/min to 80 °C	Ramp at 2 °C/min to 135 °C
80 °C Dwell for 300 mins	135 °C Dwell for 90 mins
Ramp at 2 °C/min to 20 °C	Ramp at 0.3 °C/min to 180 °C
Ramp at 2 °C/min to 80 °C	180 °C dwell for 60 mins
Ramp at 0.3 °C/min to 120 °C	Ramp at 3 °C/min to 20 °C
120 °C dwell for 120 mins	
Ramp at 3 °C/min to 20 °C	

Table 2 The enthalpy of reaction of the LTC, HTC and uncured prepreg and the resulting degree of cure of LTC and HTC MTM46 panels

	Uncured (ΔH_t)	**LTC (ΔH)**	**HTC (ΔH)**
Sample 1	122.09	46.67	22.43
Sample 2	147.17	47.01	22.77
Sample 3	137.44	47.57	22.09
Sample 4	126.64	47.73	22.50
Sample 5	133.22	50.77	22.07
Mean (Wg^{-1})	133.31	47.95	22.37
Standard deviation (Wg^{-1})	9.74	1.63	0.29
α (% cure at 250 °C)	-	64.03	83.22

Table 3 Linear coefficient of thermal expansion for UD and woven constituent plies tested at 0º and 90º for UD and 0º and 45º for woven materials cured using LTC and HTC schedules

	Linear CTE (10^{-6} ºC^{-1})	**Standard deviation**
UD-HTC-0°	-1.59	0.12
UD-LTC-0°	-1.62	0.23
UD-HTC-90°	41.04	0.02
UD-LTC-90°	56.71	0.18
W-HTC-0°	4.47	1.78
W-LTC-0°	8.56	0.61
W-HTC-45°	5.14	0.65
W-LTC-45°	9.04	1.10

Table 4 Transverse and delamination cracking temperatures of UD-LTC, UC-HTC, W-LTC and W-HTC laminates

	Mean cracking temperature	Standard deviation	Minimum	Maximum
Units	°C	°C	°C	°C
$UD\text{-}LTC_{Transverse}$	-59.8	11.4	-83.1	-49.5
$UD\text{-}LTC_{Delamination}$	-61.8	17.1	-73.4	-52.5
$UD\text{-}HTC_{Transverse}$	-72.9	11.4	-77.0	-64.8
$UD\text{-}HTC_{Delamination}$	-33.9	40.0	-76.3	11.2
$W\text{-}LTC_{Transverse}$	-74.4	11.4	-83.0	-50.4
$W\text{-}HTC_{Transverse}$	-71.5	17.1	-81.7	-41.7